Conference Paper, Published Version

Aniel-Quiroga, Íñigo; Vidal, César; Lara, Javier L.; González, Mauricio

Analysis of the Pressures in the Crown-Wall of Rubble-Mound Breakwaters under Tsunami Actions, Based on Laboratory Experiments

Coastal Structures 2019 - Nils Goseberg, Torsten Schlurmann (eds) - © 2019 Bundesanstalt für Wasserbau
ISBN 978-3-939230-64-9 (Online) - DOI: 10.18451/978-3-939230-64-9_024

Analysis of the Pressures in the Crown-Wall of Rubble-Mound Breakwaters under Tsunami Actions, Based on Laboratory Experiments

Í. Aniel-Quiroga, C. Vidal, J. L. Lara & M. González
Environmental Hydraulics Institute, Universidad de Cantabria - Avda. Isabel Torres, 15, Parque Científico y Tecnológico de Cantabria, 39011, Santander, Spain

Abstract: The stability design of crown-walls of rubble-mound breakwaters traditionally depends on the expected storm wave load history along its life cycle. However, tsunami wave loads in a crown-wall can definitely exceed the ones considered for storm waves. The existing design methods for crown-walls (e.g. Martin et al., 1999; Pedersen and Burcharth, 1992) were developed to be applied to crown-walls exposed to wind-waves but tsunamis fall out of their application range, due to its characteristics. In this study, as part of the project FP7 ASTARTE, focused on describing and understanding the pressures that this super-structures must deal with in case of a tsunami. This study is the continuation of our previous work, Aniel-Quiroga et al. (2018), where the experiments were presented and the results of rubble-mound breakwaters stability (with and without crown-wall) under tsunami actions were analyzed.

Keywords: Rubble-mound breakwater, lab experiments, tsunami actions, solitary wave, pressures, crown-wall

1 Introduction and Motivation

The 2004 event in the Indian Ocean set a watershed in tsunami science. Synolakis & Bernard (2006) highlighted this statement stablishing, within a global approach to the tsunami science, the two main aspects to be addressed when tackling tsunami risk reduction: “The determination of the inundation and run-up of tsunamis and forces on coastal structures is one of the quintessential problems in tsunami hazard mitigation”. This second important aspect of the tsunami science is the main object of the study.

In case of tsunami, marine structures stand as the first defense barrier at the coastline, and, thus, they play an important role in the mitigation of tsunami wave impacts (Takagi et al. 2014). As an example, Tomita et al. (2012) presented a work developed after the 2011 tsunami event in Japan, in which the presence of harbor structures at Kamaishi port played an active role in decreasing the destructive effect of the tsunami wave. Although breakwaters at Kamaishi port were partially destroyed, they delayed the arrival of the wave to land by six minutes, reducing the inundation area considerably, and helping in the evacuation of the population. The response of vertical structures has already been addressed by several authors, e.g. Asakura et al. (2002), Kato et al. (2006), Mizutani and Imamura (2001). However, the effectiveness and stability of rubble-mound breakwaters (RMBs) during tsunami events have not been sufficiently studied.

Rubble-mound breakwaters are commonly constructed with a parapet or crown-wall. These superstructures have several functions, such as allowing rolled access for functional or maintenance reasons, overtopping reduction or back slope armor protection. The crown-wall stability design depends on the expected wave load history during its service life. It is common to link these loads to a design-storm, given by its significant wave height and peak period. However, the loads that a tsunami can cause are not often considered in the design stage of the crown-wall.

Regarding wind waves, there are several methods to calculate the forces on crown-walls. Iribarren and Nogales (1964) calculated the horizontal forces on the crown wall, following a graphical method. Günbak (1985) split the effect of the impinging wave in two components: a dynamic part considering the impact of the wave on the crown-wall and a hydrostatic part. This separation of components was upgraded by other authors based on laboratory experiments. Firstly, Pedersen and Burcharth (1992) studied the influence of other variables in the forces on the crown-wall, like significant wave height, wavelength, berm width, etc... Secondly, Martín et al. (1995 and 1999), highlighted the necessity of calculating both components, since their origins are different and they do not occur simultaneously.

However, the performance of crown-walls in case of tsunami is out of the range of application of these existing methods due to the fact that tsunamis are extremely long waves, they propagate always in shallow waters, and they do not reach the coast always as a bore. Harbitz et al. (2016), and Guler et al. (2015), conducted laboratory experiments on RMB with crown-walls. In their experiments, the crown-wall slid or turned due to the tsunami actions. Although the real effect was well represented, they could not record the complete pressure series. In this study, we conducted lab tests on RMB, but we did not allow the crown-wall to move, so the final pressure was recorded at each scenario, fostering a further analysis of the pressures that these kinds of structures must deal with in case of tsunami.

Section 2 shows a description of the laboratory experiments, including the characteristics of the tested structure, the wave generation method, and the instrumentation installed. Section 3 describes some already obtained results based on recorded data during experiments and section 4 draws some conclusions of the study.

2 Laboratory experiments

The tested RMB was defined to represent a classical design and dimensions of a breakwater in a marina in the Mediterranean Spanish coast (MOPU, 1988). These marina breakwaters are mainly built in shallow areas using quarry stones. The slopes are usually 1/3 to ensure quarry stone stability. They are designed with a low crest, sometimes with a crown-wall on top, with most of them being overtopped during large storm events. This aspect makes these structures highly vulnerable in a potential tsunami event.

Fig. 1. IHCantabria flume in Santander, Spain

Experiments were performed at the University of Cantabria (Spain) facilities. The COCOTsu (Wave-Current-Tsunami) flume located at the Environmental Hydraulics Institute (IHCantabria) laboratory was used (see Fig. 1).

The flume is 52 m long, 2 m wide and 2.5 m high. Model structure was built inside the 24-m long testing area with transparent side walls and bottom. The flume is equipped with a 2 m-stroke piston wavemaker capable of generating long waves as the ones used in the present tests. At the same time, this facility is also capable of generating currents due to a pumping system that can work under wave action. The flume's bottom is not horizontal. It is 0.35 m deeper at the wavemaker location than at the test area. A 1/13.5 sloped ramp connects both sections, as shown in Fig. 2. Tests were performed using a water depth of 0.4 m on the testing section (0.75 m at the wavemaker).

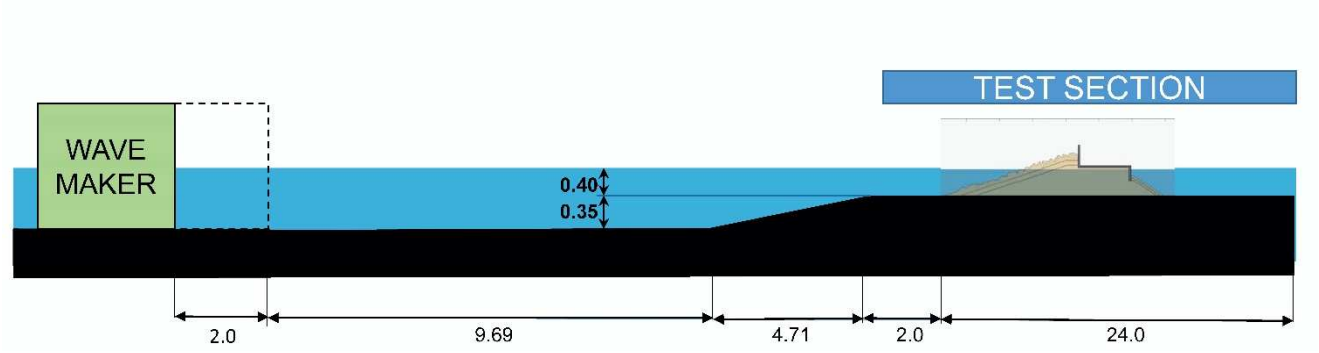

Fig. 2. IHCantabria flume scheme

2.1 *Description of the tested structure*

RMB model was built at a 1/20 scale. Froude scale laws were used to model waves and currents. The breakwater was built on the testing section of the flume at a depth of 40 cm (8 m in the prototype). The outer slope of the armor for both breakwaters was 1/3. Inner armor slopes were 1/1.5 and armor units consisted of quarry stones with a density of ρ_s=2650 Kg/m^3.

The breakwater's outer layers were calculated to have stable armor units for the seaside slope considering a sea state with H_s=6 m and T_p=10 s. The model was defined with a 23 cm wide (4.6 m in the prototype) upper berm located 25 cm (5 m in the prototype) above still water level (SWL). The crown-wall's crest height was 35 cm (7 m in the prototype) above the SWL and it included a 77 cm (15.4 m in the prototype) wide access road located 5 cm above SWL (1 m in the prototype). The crown-wall model was made of plywood and it was fixed to the flume bed using steel bars to avoid sliding. It was built using three gravel types, whose characteristics are detailed in Fig. 3.

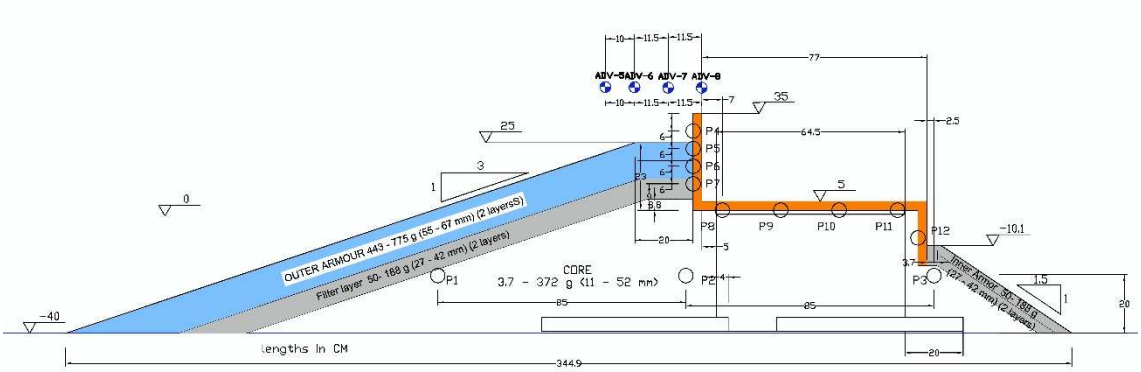

Fig. 3. Transversal section of the RMB model with crown-wall. P: pressure gauges. ADV: acoustic velocimeters. Elevations are referred to the initial water level. Dimensions in cm

2.2 *Generation of tsunami-like waves in the lab*

Solitary waves have been frequently used in laboratory experiments to simulate tsunami waves (Synolakis 1987; Jayaratne et al. 2013). However, tsunami wave hydrodynamics are somehow incomplete using solitary waves (Madsen et al. 2008) since the "tail" of the tsunami, which propagates after the wave crest, is not included in the solitary wave shape. Recent studies have proposed more sophisticated approaches based on the use of different wave profiles, as discussed by Kanoglu et al. (2015). Accordingly, Rossetto et al. (2011) and Goseberg et al. (2013) used a pneumatic and a pump-driven wave maker, respectively, to get a better representation of tsunami wave profiles measured in the field. More recently, Schimmels et al. (2016) generated more realistic wave profiles using real

tsunami records generated with a piston type wavemaker, improving tsunami wave representation. Although important improvements have been made in the last years, none of them can provide yet a complete representation of the whole tsunami wave, especially at a large scale. Due to the unfeasibility of reproducing the full tsunami length, in these experiments the tsunami wave was reproduced simulating first wave impacts and the wave overflow separately.

Fig. 4. Solitary wave impacting on RMB. Solitary wave height at the toe of the RMB model: 0.38 m

First wave impact was simulated by means of solitary waves. Six solitary wave load cases, were generated in the laboratory varying wave height at the generation area from 0.20 m to 0.45 m, with a 5 cm interval (see Tab. 1).

Tab. 1. Solitary wave experiments. Tests were performed using a water depth of d=0.4m on the testing section (0.75m at the wavemaker).

	Solitary wave height (m)				
	Model			**Prototype**	
Test	**Generation**	**Toe**	**H/d**	**Generation**	**Toe**
SW1	0.20	0.22	0.55	4.0	4.4
SW2	0.25	0.28	0.7	5.0	5.6
SW3	0.30	0.33	0.825	6.0	6.6
SW4	0.35	0.38	0.95	7.0	7.6
SW5	0.40	0.43	1.075	8.0	8.6
SW6	0.45	0.48	1.2	9.0	9.6

Tsunami overflow tests were carried out using the flume recirculation pumping system. An overflow current was generated to induce a different water level at both sides of the structure. The water level gradient at the breakwater's sides triggered overtopping over the breakwater' crest

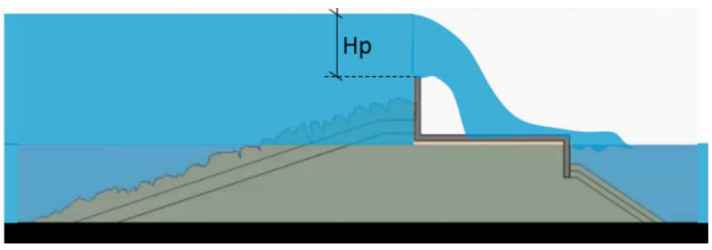

Fig. 5. Scheme of the landward area during current tests. Hp is the maximum overflow peak, used as characteristic variable of each experiment

2.3 Instrumentation

Free surface, pressure and velocity were measured for both types of experiments (solitary waves and overflow). The location of the installed gauges is given in Fig. 6. Fig. 7 shows the exact location of the pressure gauges installed in the crown-wall. Pressure transducers sampling frequency was 100 Hz.

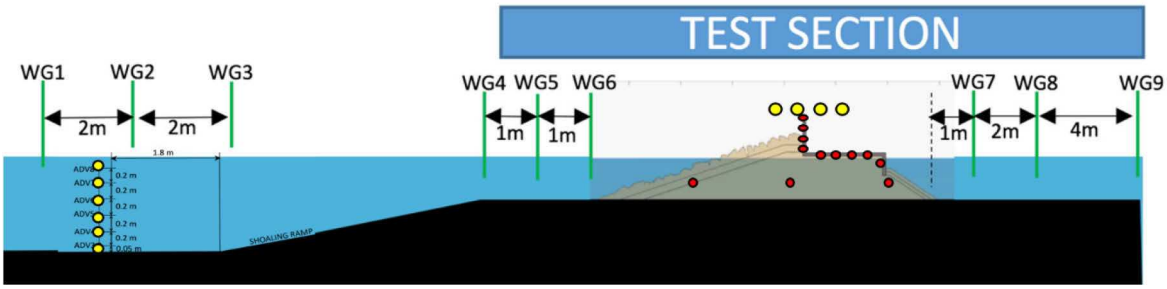

Fig. 6. Scheme of the location of the installed instrumentation. Yellow: ADVs; red: Pressure Gauges; WG: free surface gauges

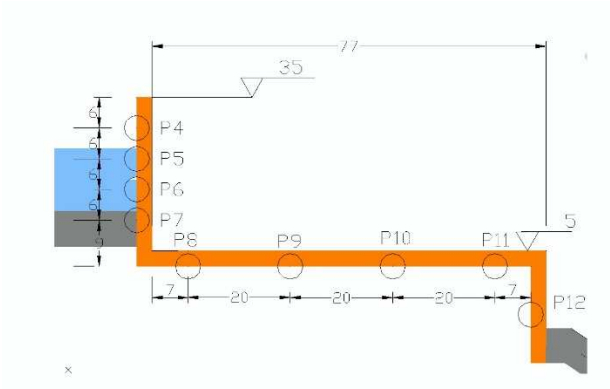

Fig. 7. Location of the pressure gauges that were placed in the crown-wall

3 Obtained results

The performed laboratory experiments and the installed instrumentation allowed analyzing the loads that a crown-wall faces when it is hit by tsunami-like actions.

For each test, pressures on each gauge were recorded. With these data the resultant forces in the vertical and horizontal parts of the crown-wall were calculated focused on evaluate whether forces balance in the crown-wall could trigger its sliding or overturning. This balance was assessed by means of a safety margin that is explained later in this section.

The loads that the crown-wall supports, and, consequently its performance varied from solitary waves to overflow currents tests. Following, some representations of the recorded and calculated variables are given.

3.1 Solitary wave experiments

Pressure time series represent the evolution of pressure with time, recorded at each gauge. Fig. 8 shows the pressure time series for a solitary wave of 0.35 m.

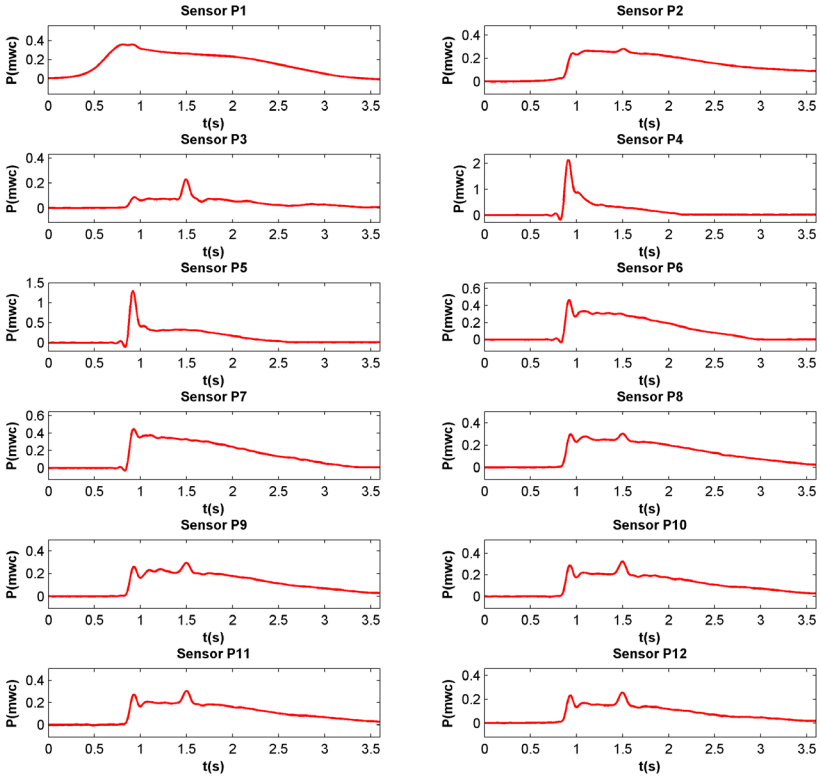

Fig. 8. Pressure time series of a solitary wave of 0.35 m high. Pressure is given in meter-water-column (mwc).

Sensors P1, P2 and P3 were placed inside the core. They showed a gradual rise, following the water level increase caused by the wave arrival.

Sensors P4, P5, P6 and P7 were located in the vertical wall of the crown-wall, being the part that receives the direct impact of the solitary waves. Among them, and due to the berm disposition, P4 is the only pressure sensor that is completely exposed to the impact of the wave. Sensor P5 is in the limit of the berm marking a transition from pressures in protected to non-protected areas. Sensors P6 and P7 are completely covered by the seaside slope armor layer, and thus they are protected from the direct action of the wave. As a consequence, pressure peak on P4 is higher than in P5 and the pressure in the latter one is higher than in P6 and P7.

Sensors P8 to P11 were placed in the horizontal part of the crown-wall to record the uplift pressures and forces during the tests. The time series of these sensors have the same shape for the each solitary wave height, and the pressures decrease from seaside to leeside gauges.

3.2 Overflow current experiments

For the case of overflow current tests, the pressure laws followed exactly the water level rise and decrease. Fig. 9 shows the pressure laws recorded at each sensor for a experiment where the *Hp* (maximum peak overflow height) reached 14 cm (2.8 m in prototype). Maximum pressures for each overflow current experiment was recorded at sensor P4, but they were in general lower than pressure on solitary wave experiments.

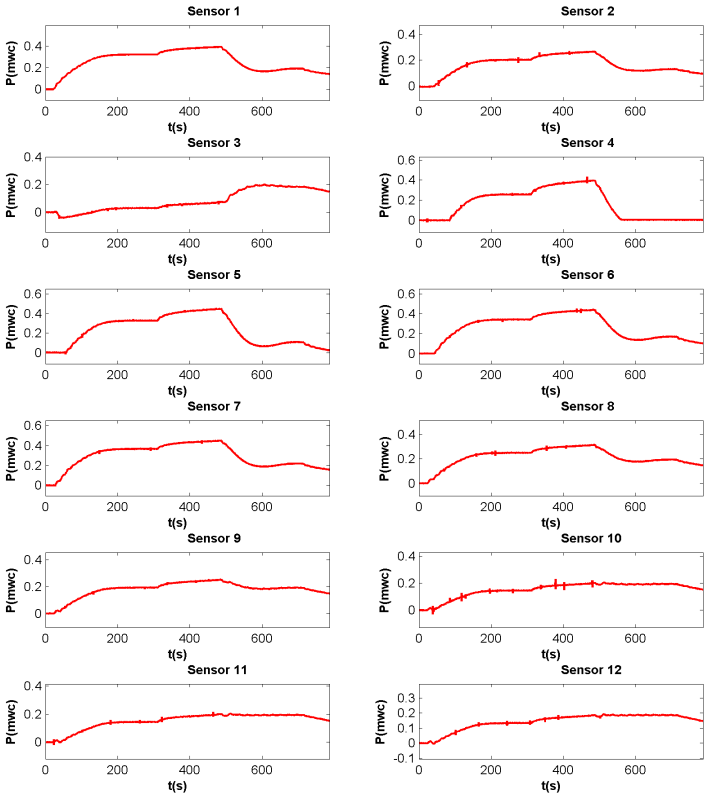

Fig. 9. Pressure time series of a standard current test. Pressure is given in meter-water-column (mwc)

3.3 Resultant forces

Using the pressure records on each sensor the resultant forces in the vertical and horizontal parts of the crown-wall were calculated focused on evaluate whether the crown-wall forces balance could trigger a structural failure. Two failure modes of the crown-wall have been studied: sliding and overturning. The failure conditions have been assessed by means of margins of safety. These margins were considered as the deficit among stabilizing and destabilizing forces and moments. The minimum the margins, the closer to the failure the structure is.

A simplified balance of forces and moments in the crown-wall is shown in Fig. 10.

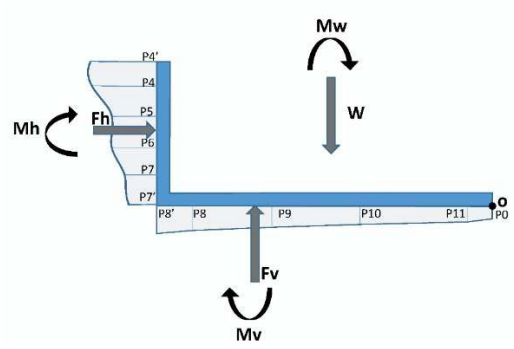

Fig. 10. Scheme of the equilibrium of forces acting on the crown wall. F_h: Resultant of the horizontal forces. F_v: Resultant of the vertical forces. W: weight of the crown-wall. M_h, M_v, M_w: Moments of F_h, F_v and F_w, respectively.

Pressures were integrated to obtain the resultant forces both in the horizontal (F_h) and the vertical (F_v) parts of the crown-wall. To complete the pressure law at horizontal and vertical parts P4', P7', P8'(~P7') and P0 where obtained by linear extrapolation of the neighbor gauges.

The margins of safety for sliding (S_s) and overturning (St) failures were formulated as follows:

$$S_s = \mu \cdot W - \mu \cdot F_v - F_h$$

$$S_t = M_w - (M_v + M_h)$$

where W is the weight of the crown-wall, F_v and F_h are the resultant forces on the vertical and horizontal parts, M_v and M_h are the moments of those resultants at point O (see Fig. 10) and μ is the friction coefficient. Several authors (Hamilton & Hall, 1992; Jensen, 1984; Goda, 2000) discussed the value of μ between concrete superstructures and quarry stone, finding that it is around 0.5-0.6. In this analyses, a value of 0.5, as used also by Allsop et al. (1996), has been applied.

The weight does not vary with time and therefore, the minimum S_s and S_t is determined by the maximum value of $(\mu \cdot F_v + F_h)$ and $(M_v + M_h)$

In Fig. 11, the F_h, F_v and their balance $(\mu \cdot F_v + F_h)$ time series are given for a 0.35 m solitary wave.

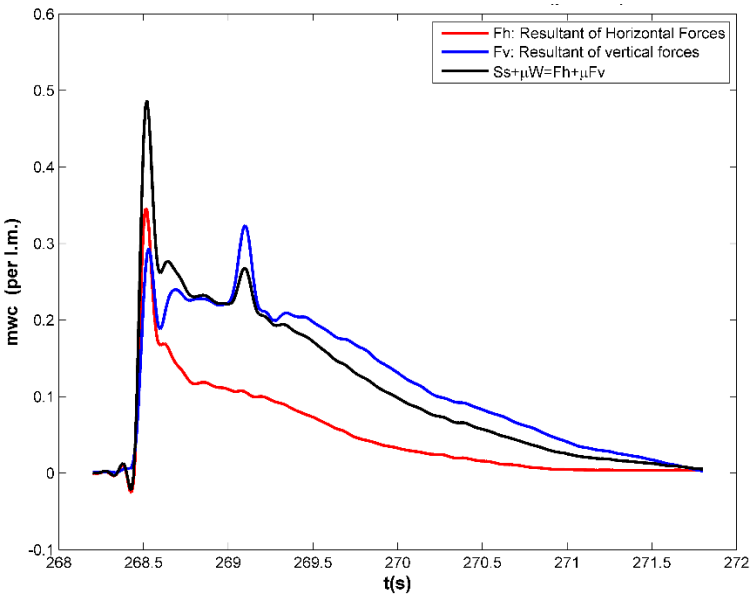

Fig. 11. Time evolution of forces resultant for a 0.35 m high solitary wave. Pressure units are meters of water column (mwc). The factor Fh+μFv (in black) represents the maximum pressure per linear meter in that test. The instant of Its maximum value is the same as the instant of the minimum margin of safety Ss.

In solitary waves experiments, F_h curve follows a similar shape as the pressure time series on the sensors located on the vertical part of the crown-wall the dynamic first peak (impact) is followed by a secondary smaller peak, result of the water accumulated by the crown-wall, and the run-down process, and linked to a static or pseudo-static load. After that, a steady decline of the horizontal force is observed.

F_v or uplift curve shows also a dynamic first peak but it is much smaller than in the case of F_h. After that, the second peak is noted, again as a consequence of the evolution of the wave. Except in the first part of the curve, F_v is bigger then F_h. This is due to the fact that the horizontal part of the crown-wall is much longer than the vertical one, and consequently, the integrated value of the resultant is affected by this aspect.

The evolution of the sliding margin of safety (S_s) shows a first dynamic peak, result of the contribution of F_h to S_s, and a second and smaller peak, caused by the pseudo-hydrostatic load of the solitary wave on the crown-wall.

Fig. 12a shows the comparison of the time series of Ss for each wave height. Fig. 12b shows the same curve but related to St, where a similar tendency is observed. In this figures, the dynamic peak is always the greatest force. In the experiments with lower wave height (SW1 and SW2), the pseudo-static peak is similar to the first one, but the difference between those peaks grows with the height, and the steepness, as explained in Takahasi (Takahashi 2009).

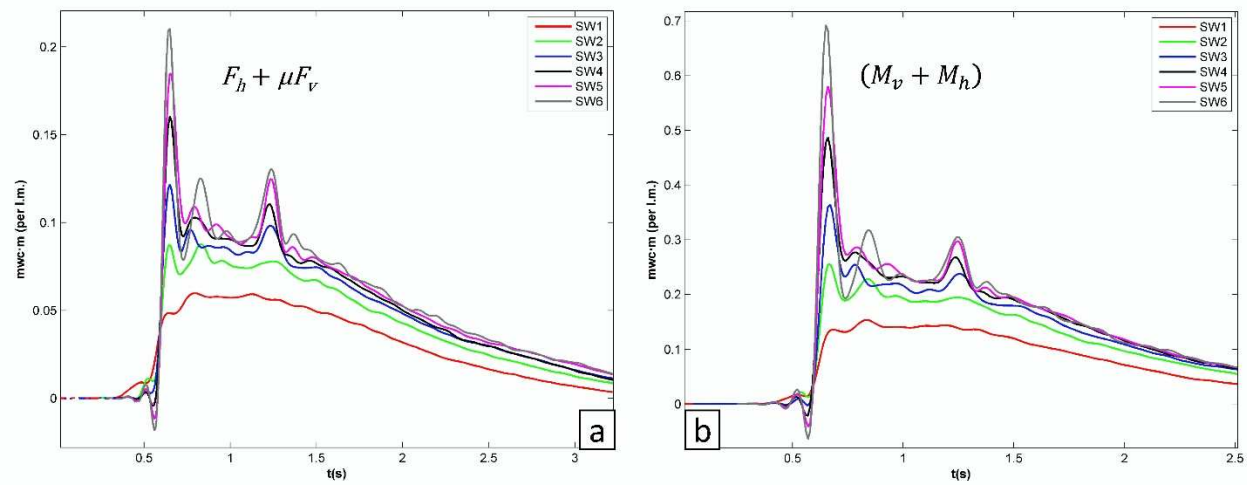

Fig. 12. (a) Time evolution of Fh+μFv in mwc per linear meter. (b) Time evolution of Mv+Mh for each tsunami wave height. Units are meters of water column mwc·m per linear meter. Curves have been overlapped to make it easier the comparison.

Regarding the overflow current experiments, Fig. 13 shows the time evolution of F_h, F_v, and S_s for one of the tests. In this case, the resultant forces curves follow mimetically the records of the gauges. The margins of safety do not present fluctuations but a gradual increase, in parallel to the overflow height rise. The maximum values of the resultants and the more limiting values of the margins of safety of the overflow current tests were all lower than the peak values in solitary waves set, except for the lowest wave SW1.

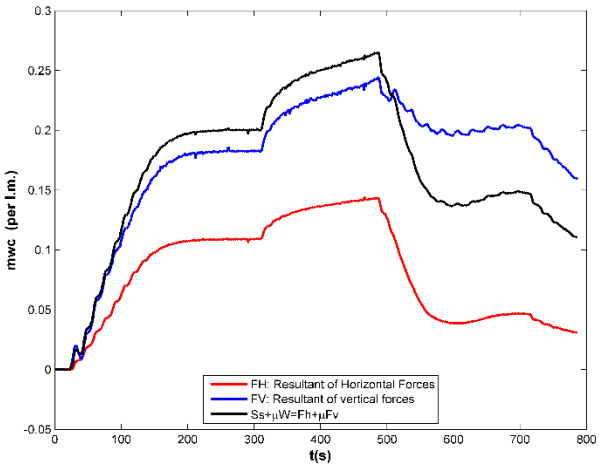

Fig. 13. Time evolution of forces resultant for the overflow current test Q28. Pressure units are meters of water column (mwc). The factor Fh+μFv (in black) represents the maximum pressure per linear meter in that test. The instant of its maximum value is the same as the instant of the minimum margin of safety Ss.

4 Conclusions

Regarding the pressures recorded in the tsunami-structure interaction, several conclusions can be stated:

- The initial dynamic impact produces the largest pressures in the vertical part of the crown-wall
- Pressure in the protected and non-protected parts of the corwn-wall are in a relation 1:3
- In the experiments with lower wave height (SW1 and SW2), the pseudo-static peak is similar to the dynamic one
- For the range of waves tested, the pressures produced by the overflow current overtopping the structure are lower than the initial dynamic impact of the tsunami.

Acknowledgements

The research leading to these results has received funding from the European Union's Seventh Framework Programme (FP7/2007-2013) under grant agreement n° 603839 (Project ASTARTE - Assessment, Strategy and Risk Reduction for Tsunamis in Europe).

References

Asakura, R. et al., 2002. The tsunami wave force acting on land structures. In *Proceedings of the 28th International Conference on Coastal Engineering, ASCE*. pp. 1191–1202.

Goda, Y., 2000. Random Seas and Design of Maritime Structures, Available at: www.worldscientific.com [Accessed November 9, 2017].

Goseberg, N., Wurpts, A. & Schlurmann, T., 2013. Laboratory-scale generation of tsunami and long waves. *Coastal Engineering*, 79, pp.57–74. Available at: http://dx.doi.org/10.1016/j.coastaleng.2013.04.006.

Guler, H.G. et al., 2015. Performance of rubble mound breakwaters under tsunami attack, a case study: Haydarpasa Port, Istanbul, Turkey. *Coastal Engineering*, 104, pp.43–53. Available at: http://dx.doi.org/10.1016/j.coastaleng.2015.07.007.

Günbak, A., 1985. Damage of Tripoli harbor north west breakwater. In P. Bruun, ed. *Design and construction of mounds for breakwaters and coastal protection*. Elsevier, pp. 676–695.

Hamilton, D.G. & Hall, K.R., 1992. Preliminary Analysis of the Stability of Rubblemound Breakwater Crown Walls. In ASCE, ed. *Coastal Engineering Proceedings*. Venice, Italy: Council on Wave Research, the Engineering Foundation. Available at: https://journals.tdl.org/icce/index.php/icce/article/view/4770/4451 [Accessed July 7, 2017].

Harbitz, C.B. et al., 2016. Risk Assessment and Design of Prevention Structures for Enhanced Tsunami Disaster Resilience (RAPSODI)/ Euro-Japan Collaboration. *Coastal Engineering Journal*, 58(4). Available at: www.worldscientific.com [Accessed April 12, 2017].

Iribarren, R. & Nogales, C., 1964. *Obras Marítimas* Dossat, ed., Madrid.

Jayaratne, R. et al., 2013. Investigation of Coastal Structure Failures due to the 2011 Great Eastern Japan Earthquake Tsunami. In *Coasts, Marine Structures and Breakwaters 2013*.

Jensen, J., 1984. *A monograph on rubble mound breakwaters*, Danish Hydraulic Institute (DHI).

Kanoglu, U. et al., 2015. Tsunamis: bridging science, engineering and society. *Philosophical Transactions of the Royal Society*, 373, pp.1–24.

Kato, F., Inagaki, S. & Fukuhama, M., 2006. Wave force on coastal dike due to tsunami. *Coastal Engineering*, pp.5150–5161. Available at: http://pwweb1.pwri.go.jp/eng/ujnr/joint/37/paper/13kato.pdf.

Madsen, P.A., Fuhrman, D.R. & Scha, H.A., 2008. On the solitary wave paradigm for tsunamis. *Journal of Geophysical Research*, 113(December).

Martín, F.L. et al., 1995. Un Método para el Cálculo de las Acciones der Oleaje Sobre los Espaldones de los Diques Rompeolas. *Ingeniería del Agua.*, 2(3).

Martin, F.L., Losada, M.A. & Medina, R., 1999. Wave loads on rubble mound breakwater crown walls. *Coastal Engineering*, 37(2), pp.149–174.

Mizutani, S. & Imamura, F., 2001. Dynamic wave force of tsunamis acting on a structure. *ITS 2001 Proceedings*, (7), pp.941–948.

Pedersen, J. & Burcharth, H.F., 1992. Wave Forces on Crown Walls. *Coastal Engineering Proceedings*, 1(23).

Rossetto, T. et al., 2011. Physical modelling of tsunami using a new pneumatic wave generator. *Coastal Engineering*, 58(6), pp.517–527. Available at: http://www.sciencedirect.com/science/article/pii/S0378383911000135.

Schimmels, S., Sriram, V. & Didenkulova, I., 2016. Tsunami generation in a large scale experimental facility. *Coastal Engineering*, 110, pp.32–41. Available at: http://www.sciencedirect.com/science/article/pii/S0378383915002136 [Accessed May 17, 2017].

Synolakis, C.E., 1987. The runup of solitary waves. *Journal of Fluid Mechanics*, 185(1), p.523.

Synolakis, C.E. & Bernard, E.N., 2006. Tsunami science before and beyond Boxing Day 2004. *Philosophical Transactions of the Royal Society A: Mathematical, Physical and Engineering Sciences*, 364(1845), pp.2231–2265. Available at: http://rsta.royalsocietypublishing.org/content/364/1845/2231.abstract.

Takagi, H. et al., 2014. Assessment of the effectiveness of general breakwters in reducing tsunami inundation in Ishinomaki. *Coastal Engineering Journal*, 5621(4). Available at: www.worldscientific.com [Accessed May 31, 2017].

Takahashi, S., 2009. Development of Caisson Breakwater Design based on failure experiences. *Handbook of Coastal and Ocean Engineering*, pp.455–478.

Tomita, T. et al., 2012. Breakwater Effects on Tsunami Inundation Reduction in the 2011 off the Pacific Coast of Tohoku Earthquake. *Journal of Japan Society of Civil Engineers, Ser. B 2(Coastal Engineering)*, 68(2), pp.4–8.